IMMUNOCYTOCHEMICAL LOCALIZATION OF A LARGE INTRINSIC MEMBRANE PROTEIN TO THE INCISURES AND MARGINS OF FROG ROD OUTER SEGMENT DISKS

DAVID S. PAPERMASTER, BARBARA G. SCHNEIDER, MARK A. ZORN, and JEAN P. KRAEHENBUHL

From the Departments of Pathology and Cell Biology, Yale University School of Medicine, New Haven, Connecticut 06510, and the Institute of Biochemistry, University of Lausanne, Lausanne, Switzerland

ABSTRACT

Immunocytochemical techniques have localized a large protein which is an intrinsic membrane component of isolated frog rod outer segments (ROS). This large protein whose apparent mol wt is 290,000 daltons comprises about 1–3% of the ROS membrane mass. Its molar ratio to opsin is between 1:300 and 1:900. Adequate immune responses were obtained with <30 μg (100 pmol) of antigen per rabbit. Antibodies to the large protein were used for its localization on thin sections of frog retina embedded in glutaraldehyde cross-linked bovine serum albumin (BSA). Specifically bound antibodies were detected by an indirect sequence with ferritin-conjugated antibodies. This technique detected the protein which is represented by 1,000–3,000 molecules per disk. This indicates that the procedure is sufficiently sensitive for analysis of membrane components in low molar proportions. The large protein was specifically localized to the incisures of ROS disks which divide the disks into lobes and to the disk margin. Thus, opsin is mobile within the membrane of the disk while the large protein is apparently constrained to the disk edges. This finding raises the possibility that special functions are also localized to this unusual region of high curvature, and that collisions of bleached opsin with these edges are physiologically important in outer segment function.

KEY WORDS immunocytochemistry · retina · rod outer segments · membranes

Outer segment membranes of rod photoreceptor cells are the site of photon capture and initiation of excitation in the retina (17, 30). The membranes of rod outer segments (ROS) are arrayed as a stack of disks enveloped by a plasma membrane which is not in continuous contact with the disk lipid bilayer except at the base of the ROS (2, 6, 8). The disks of vertebrate ROS are variably cleaved into enclosed lobes by incisures (Fig. 1). Rodents and cattle usually have a single incisure which may arborize in the center of the disk (8). Primate disks have shallow scalloped borders which are associated in the incisures, to a varying extent, with microtubules (5, 34). Similar scalloping of frog ROS disks is accentuated by the penetration of the incisures nearly to the disk center (Fig. 2). However, no tubules are seen on

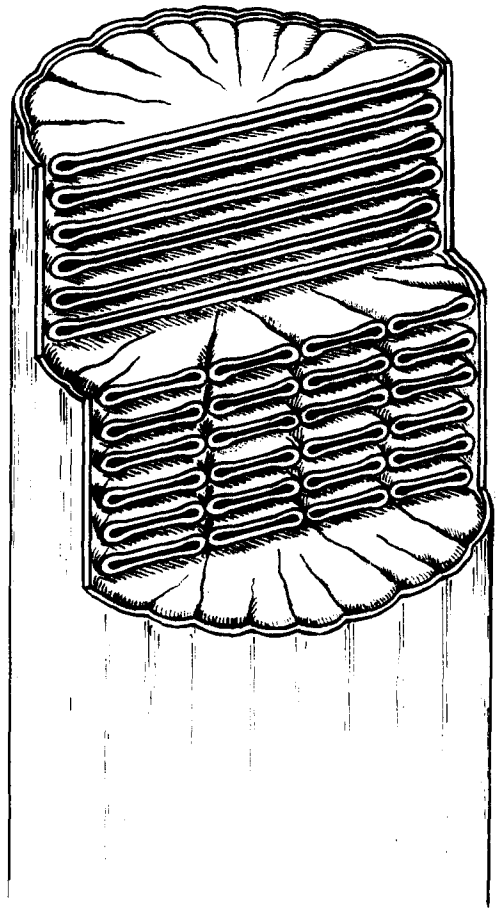

FIGURE 1 Diagrammatic representation of relationships of ROS disks and the surrounding plasma membrane of frog retina. Cross sections in the plane of the disk reveal radially oriented incisures. Longitudinal sections off-center contain multiple abutting hairpin loops of adjacent lobes of the disk in the disk interior.

cross sections beyond the connecting cilium which extends only to the lower portion of the ROS.

Proteins important in maintaining unusual geometric forms in cells, such as contractile proteins or microtubules, are usually solubilized by ionic manipulation of membranes. However, the sodium dodecyl sulfate (SDS) polyacrylamide gel profiles of isolated ROS do not indicate the presence of such proteins in large amounts in frog or cattle ROS (19, 25). Opsin, the visual pigment apoprotein, comprises about 90% of the protein mass of frog ROS (26). In addition to opsin, the next major intrinsic membrane protein component is a large molecule (about 290,000 daltons) which comprises about 1–3% of the total ROS protein

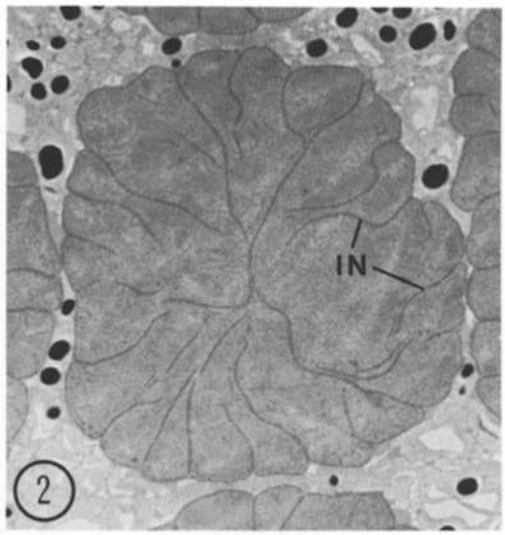

FIGURE 2 Horizontal cross section of ROS embedded in Epon. Deep invaginations of the disk membrane termed incisures (*IN*) divide the disk into lobes. × 7,000.

mass; thus, its molar ratio to opsin is between 1:300 and 1:900 (25).

This large protein is continuously synthesized and transported to ROS during disk renewal in the adult (24, 25). A comparable but smaller protein (mol wt 230,000 daltons) is found in cattle ROS. Prior immunochemical studies showed no cross-reactivity of these two proteins in contrast to the considerable immunological and molecular homology of vertebrate opsins (25). We have employed antibodies to the large protein to localize it by immunocytochemical techniques which were successful for the analysis of opsin distribution (27). This report describes the restricted binding of these antibodies to the incisures and margins of the frog ROS disk.

MATERIALS AND METHODS

Preparation of Antibodies

Rabbits were immunized with the large protein of frog ROS contained in a strip of SDS polyacrylamide gel as described previously (25). The large protein of cattle ROS was isolated electrophoretically and a protein-Sepharose immunoabsorbant was prepared by procedures previously described for preparation of a cattle opsin-Sepharose immunoabsorbant (25). Because the large protein of frog ROS membranes is available only in small amounts (e.g., 5 mg of frog ROS membranes contains <150 μg of the large protein), a specific immunoabsorbant of the frog protein has not been

prepared. Specific antisera from two rabbits were fractionated by diethylaminoethyl cellulose chromatography in 0.007 M phosphate buffer, pH 6.3, to recover the IgG fraction which was then digested with pepsin at pH 4.5 for 18 h to generate $F(ab')_2$ fragments. These antibody fragments were chromatographed on Sephadex G-150 to eliminate aggregates and concentrated as previously described for anti-opsin $F(ab')_2$ fragments (27). These products will be termed specific antibody in the remainder of the text. Yields of specific antibody were estimated by two-dimensional immunoelectrophoresis against known amounts of antigen (50 ng), and peak heights were compared to previously quantitated opsin-anti-opsin reactions (12). Before use, antisera were centrifuged at 234,000 g_{avg} (50,000 rpm, SW 50.1 rotor, Beckman Instruments, Fullerton, Calif.) for 2 h. Portions of the specific antibody to the large protein of frog ROS were absorbed with cattle protein-Sepharose and opsin-Sepharose immunoabsorbants to determine whether cross-reactions with this antigen were detectable.

Immunocytochemical Reactions on Thin Sections of BSA-Embedded Retinas

Frog retinas embedded in cross-linked bovine serum albumin (BSA) were reacted with specific antibodies as described previously (27). In addition to the formaldehyde-glutaraldehyde-fixed retinas described before, tissues fixed initially with 2% glutaraldehyde in 0.1 M phosphate buffer, pH 7.4, for 1 h were also analyzed. Second-stage reactions employing ferritin-conjugated $F(ab')_2$ of sheep anti-rabbit $F(ab')_2$ and subsequent staining with lead citrate, uranyl acetate, and bismuth subnitrate also followed the same procedures.

Morphometric Analysis and Controls

To compare localization of specific antibodies to the large protein with pre-immune sera and diluted anti-opsin antibodies, morphometric studies of the distribution of ferritin label were conducted according to the procedures described by Weibel and Bolender (32). Controls of nonimmune serum and ferritin-labeled reagents similar to our study of anti-opsin binding were employed (27).

RESULTS

Specificity of Immunochemical Reactions

Antibodies to the large protein of frog ROS react only with it and not with opsin. Peak height, a linear measure of antibody concentration (12), is unchanged by passage through immunoabsorbants of opsin or large protein of cattle ROS (Fig. 3). This indicates that these antibodies do not significantly cross-react with opsin or the cattle large protein. These results support our prior observations which showed that radiolabeled newly synthesized frog opsin was not immunoprecipitated by the antibody to the large protein of frog ROS and that the cattle and frog large proteins do not cross-react (25).

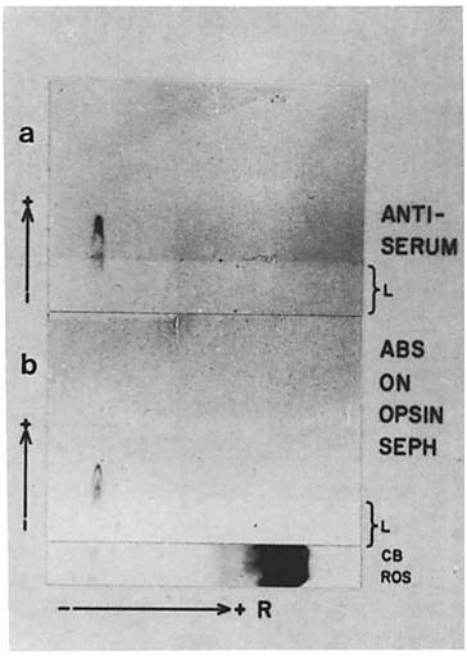

FIGURE 3 Two-dimensional immunoelectrophoretic analyses of antibodies to the large protein of frog ROS according to the technique of Converse and Papermaster (12). (*a*) Specific reactions with the large protein are limited to a narrow arc ~1 cm from the origin. Large amounts of opsin (*R*) present in the first-dimension gel are not precipitated (opsin is also not precipitated in 10- to 100-fold lower amounts). The first-dimension gel contained ~50 ng of the large protein and 5 μg of opsin. Serum concentration was 12% (vol/vol); the Lubrol PX layer (*L*) was 8 mm thick (23). The Coomassie Blue (*CB*)-stained gel below the immunoprecipitin reaction is a parallel sample containing 100 μg of ROS proteins (1 μg of the large protein) to indicate migration distances in the first dimension and relative proportion of the two ROS proteins. (*b*) After passage of the antiserum through a cattle opsin immunoabsorbant which binds precipitating anti-opsin antibodies, no significant change in arc height is observed in the specific reaction with the large protein. Comparable reactions are observed after reaction of the antiserum with an immunoabsorbant of the large protein of cattle ROS membranes.

Immunocytochemical Localization

The anatomy of frog ROS and its disks is illustrated in Fig. 1. On horizontal cross sections of ROS, the incisures appear as deep clefts which

divide the disks into lobes (Figs. 2 and 4). On longitudinal sections, the aligned incisures form a dense line in the interior of the ROS. When retinas are embedded in Epon or in cross-linked BSA, the longitudinally aligned incisures have the appearance of abutting hairpin loops within the interior of individual rods (see Fig. 2 in reference 27).

Specific antibody to the large protein labels red rod outer segments almost exclusively along incisures and disk margins (Figs. 4, 5, and 7). Individual ferritin grains are the predominant pattern of binding, but occasional clusters of about 10 ferritin grains are scattered along the aligned incisures. Usually, the clusters appear in regions of greater electron opacity, suggesting that a slightly tangential section of a group of disks has exposed more antigenic surface. Both antisera tested gave identical labeling patterns and comparable variability of labeling density with thin sections from retinas initially fixed by a formaldehyde-glutaraldehyde sequence (27) or by 2% glutaraldehyde alone.

Reactions with pre-immune sera do not result in binding of the ferritin conjugate to the incisures or disk margins (Figs. 6 and 8). The binding is therefore specific and not the result of unusual effects of the section in the region of the incisures. Cone outer segments are unlabeled to the extent that we have surveyed them. Additional controls employed in the preceding report indicate no binding of ferritin conjugates in the absence of specific antibody in the first step (27). To test the possibility that the antiserum to the large protein is simply a more dilute anti-opsin antibody, we made serial 10-fold dilutions of affinity purified anti-opsin antibody fragments. 1,000-fold and further dilutions result in progressive decrease of labeling density of the ROS, but the pattern of binding is unchanged and shows no tendency to form aligned single molecules or clusters along the incisures (Figs. 9 and 10).

Morphometric analysis by standard techniques (32) tested the probability that the apparently aligned binding of antibodies seen in Figs. 5 and 7 is really a chance result of random binding. The densities of ferritin labeling on the incisures, on disk surfaces between incisures, and on disk margins are given in Table I. The relative labeling density on incisures was two to ten times the labeling density between incisures when antiserum was used. Disk margins were also labeled with approximately one-half the density of the neighboring incisures. In comparison, 1,000-fold diluted anti-opsin showed no tendency to label incisures or margins preferentially. These results indicate that the qualitative impressions based upon micrograph appearance are supported by quantitative analysis.

DISCUSSION

The localization of the large protein to the ROS incisure and disk margin suggests that this protein does not participate in the fluid translational and rotational motions which are a characteristic of rhodopsin (3, 9, 11, 20, 28). Unlike the erythrocyte membrane which is populated with a variety of extrinsic membrane proteins whose molecular interactions are postulated to restrict intrinsic membrane protein mobility (22), the ROS membrane seems to be free of detectable amounts of extrinsic fibrous proteins (see Fig. 3 and references 19 and 26). The molecular simplicity of frog ROS membranes suggests that other proteins will exist in molar ratios of <1:1,000 compared to opsin. The large protein of frog ROS (mol wt 290,000) may be able to self-associate into this unusual region of high curvature and restrict its own further translation onto the plane of the disk. It is also possible that a minor component—per-

FIGURE 4 Horizontal cross section of retina embedded in cross-linked BSA. Sections at the level of ROS were reacted with specific antibodies to the large protein of frog ROS followed by ferritin-conjugated $F(ab')_2$ of sheep anti-rabbit $F(ab')_2$. Ferritin grains are predominantly bound to the disk margin and to the deep clefts of the incisures which divide the rod disk into multiple lobes. Dense labeling is apparent even at this low magnification. Pigment epithelial cell processes (*P*) containing dense black melanosomes surround each ROS. Bar, 1 μm. × 12,000.

FIGURE 5 Higher magnification of ROS disk labeled as in Fig. 4. Label is confined to the incisures and along the disk margin. Bar, 0.5 μm. × 34,000.

FIGURE 6 Cross section of ROS embedded in cross-linked BSA and reacted with $F(ab')_2$ antibody fragments prepared from pre-immune serum. Nonspecific labeling density is extremely low over ROS. Bar, 0.5 μm. × 34,000.

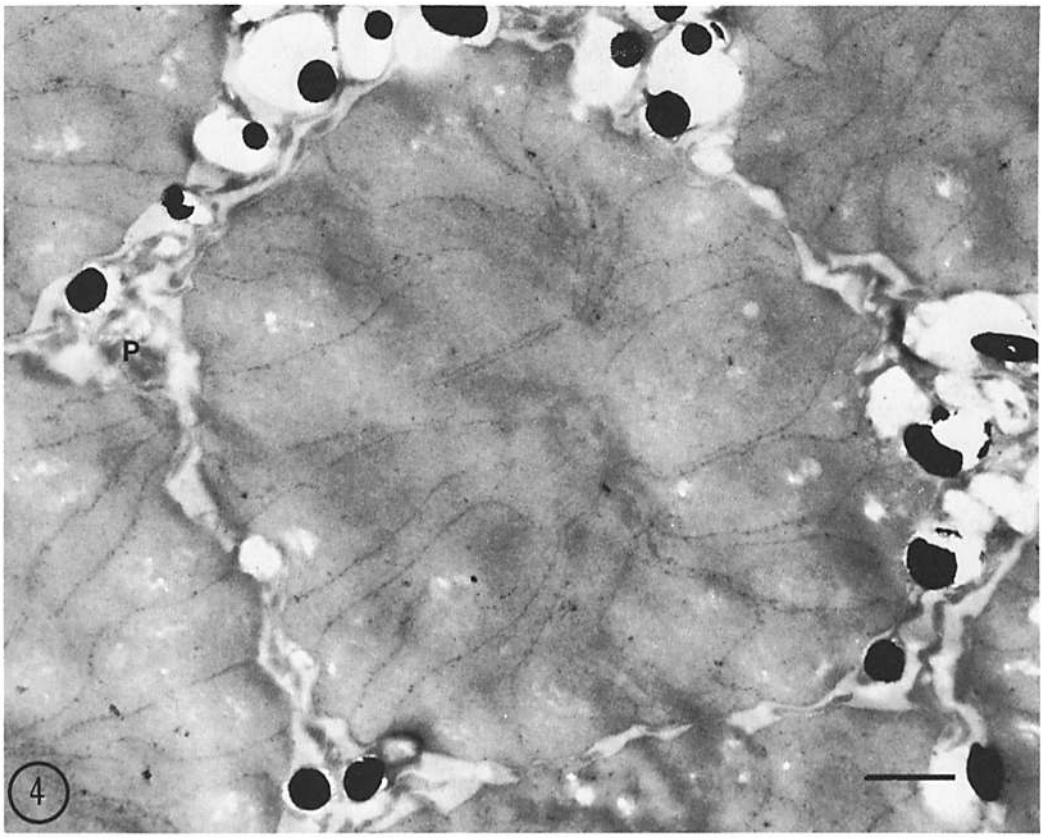
P
4

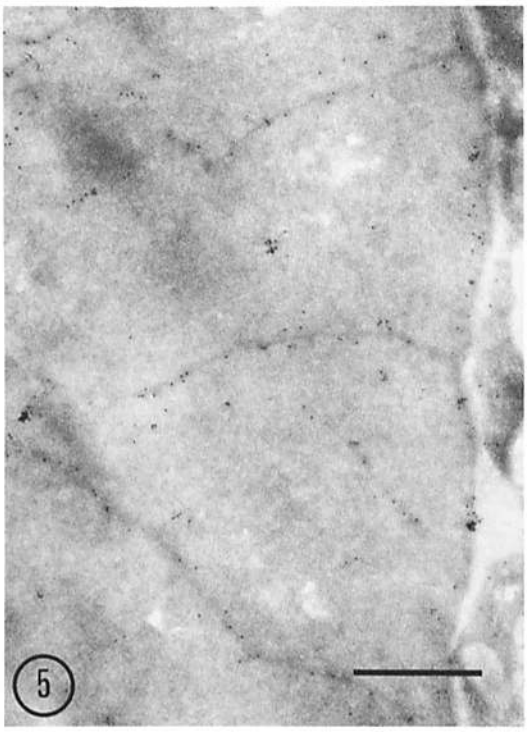
5


6

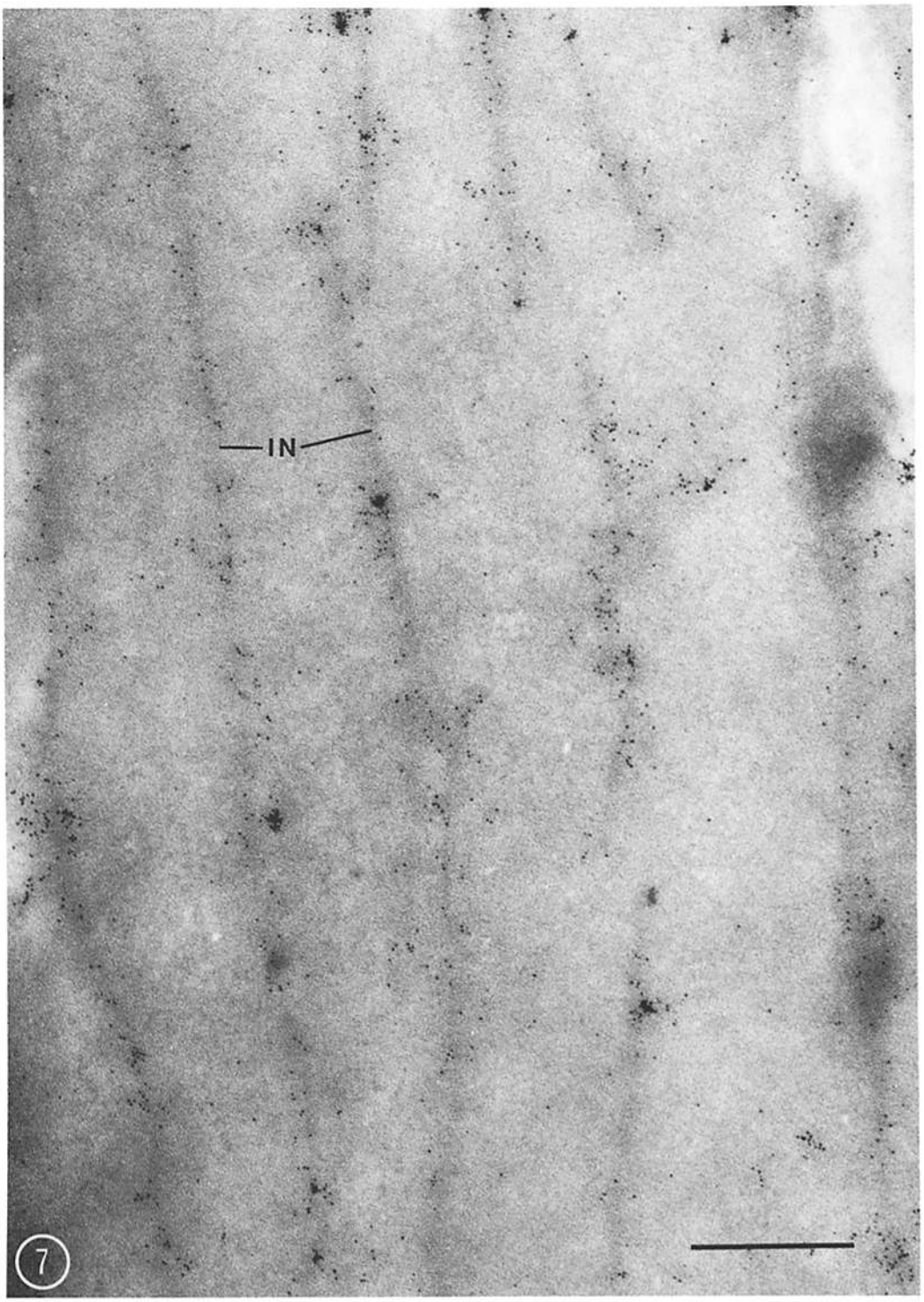

FIGURE 7 Longitudinal section of ROS reacted with the same antibodies as Figs. 4 and 5. Individual grains and small clusters of ferritin are arrayed along the longitudinally aligned edges of the sectioned incisures (*IN*) which appear as a line of higher electron opacity. Bar, 0.5 μm. × 49,000.

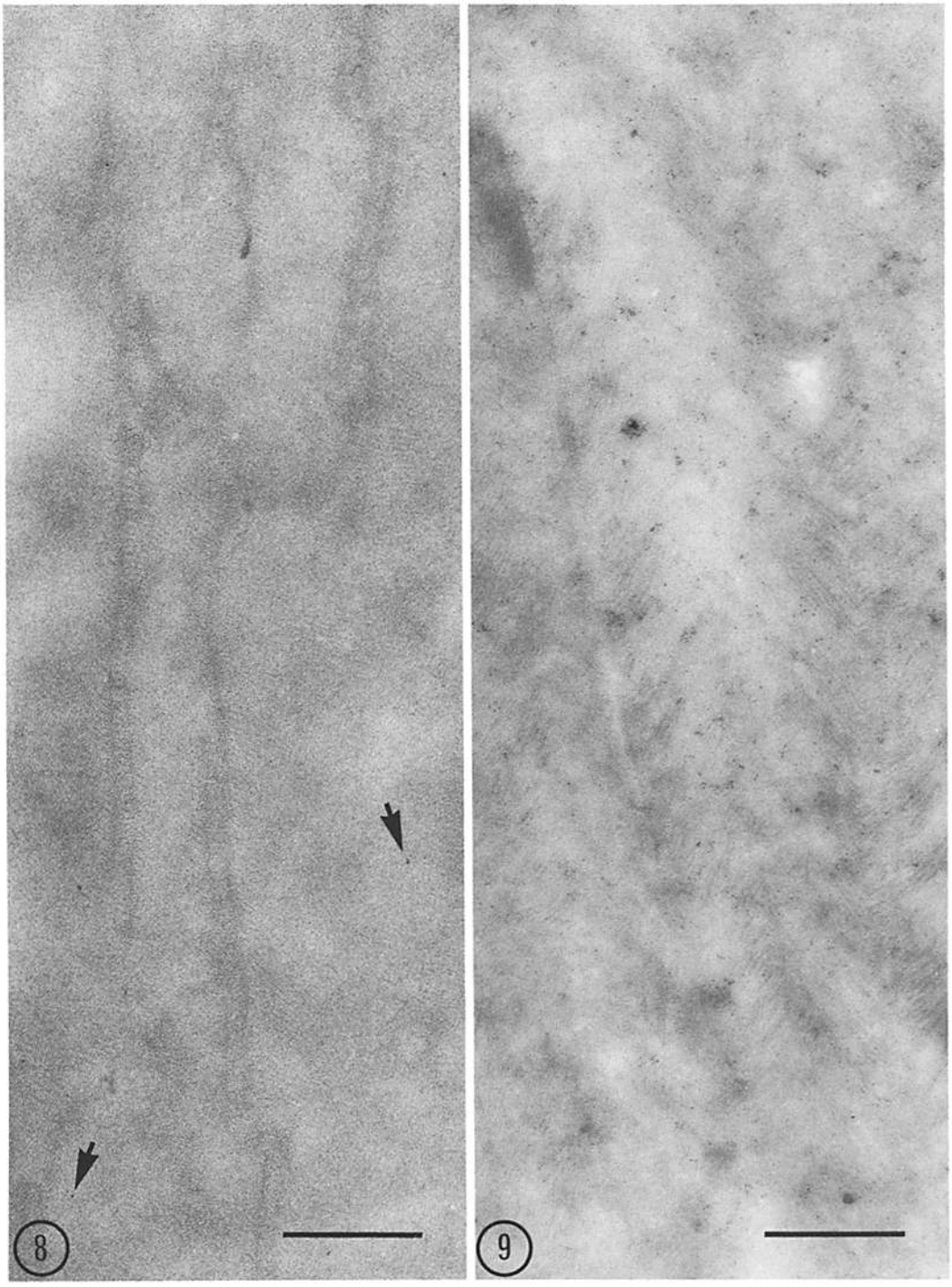

FIGURE 8 Control section of longitudinally sectioned ROS reacted with pre-immune serum $F(ab')_2$ fragments and the ferritin conjugate. Occasional ferritin grains (arrows) are scattered over the ROS but show no tendency to align with incisures. Bar, 0.5 μm. × 41,000.

FIGURE 9 Comparison of dilute anti-opsin binding. 1,000-fold dilutions of anti-opsin with pre-immune $F(ab')_2$ and 1% BSA result in a decrease in labeling density by anti-opsin to a level resembling the density illustrated in Fig. 4. However, no alignment of ferritin along the sectioned incisures is apparent. Thus, the specific reaction of antibody to the large protein along incisures and disk margins (Figs. 4, 5, and 7) is not a nonspecific artifact of the physical properties of the sectioned incisures. Bar, 0.5 μm. × 41,000.

haps nonproteinaceous – is undetected or lost during ROS isolation and has escaped molecular and biosynthetic analysis. Such a hypothetical component may stabilize the localization of the large protein to this specific site or participate in the assembly of the disk.

The incisures of all disks in an outer segment are aligned longitudinally (Figs. 1 and 7). Favorably oriented sections show no breakdown of this alignment over the entire length of >1,000 disks in the frog. Osmotically ruptured ROS or retinas fixed in hypotonic buffers under varying conditions often show swelling and disruption of disk lamellar structure, yet the edge of the disk and the incisures often remain attached to one another or

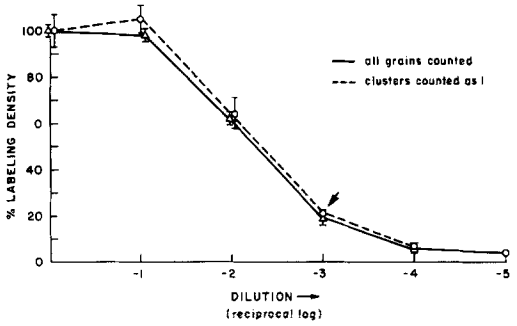

FIGURE 10 Labeling density of anti-opsin $F(ab')_2$ affinity purified antibodies on ROS. Dilution of antibody with $F(ab')_2$ fragments of pre-immune serum reduces labeling density. Fig. 9 illustrates the labeling of antibodies diluted 1:1,000 (arrow). Data illustrates mean ± SEM.

to the plasma membrane (7, 13, 16). Moreover, barium salts, in contrast to lanthanum, rarely penetrated the depths of incisures or between adjacent disks of damaged ROS. This was interpreted as an indication of some component blocking penetration which was not revealed by the usual fixatives and staining techniques (6, 7). If the large protein accounts for some of these properties, then it would play an important role in stabilizing the relationships of one disk to another and to the adjacent plasma membrane.

Restriction of the large protein to the margins of the disk and its incisures is not likely to be a result of fixation artifacts. The fixation protocol of formaldehyde followed by glutaraldehyde provides a small, rapidly penetrating fixative followed by a satisfactory cross-linking reagent. While formaldehyde did not restrict opsin's translation in the plane of the ROS disks, glutaraldehyde did inhibit both clustering of opsin molecules by antibody (18) and translation of rhodopsin across the disk after partial bleaching on one side of the ROS (20, 28). If the large protein were to become displaced from some other functional site during formaldehyde fixation, it would need to move preferentially to the incisure and disk margin before glutaraldehyde fixation. Movement induced by the bivalent $F(ab')_2$ antibody fragments would most likely be restricted by the prior glutaraldehyde treatment. Nonetheless, movement during formaldehyde fixation is not excluded. Glutaraldehyde fixation alone (Figs. 4–8) gave results identical in distribution to those of sections of

TABLE I

Ferritin-Labeling Densities over Incisures and Disk Margins of Frog ROS

	Incisures	Disk surface between incisures	Disk margins
Longitudinal Sections			
Antibody			
Exp 1 (13)	186 ± 14	25 ± 5	
Exp 2 (14)	53 ± 5	20 ± 3	
Pre-immune serum			
Exp 1 (13)	2 ± 1	3 ± 1	
Exp 2 (11)	25 ± 7	28 ± 6	
Anti-opsin 1:1000 (9)	65 ± 5	76 ± 14	
Transverse Sections			
Antibody (10)	63 ± 5	6 ± 2	32 ± 6
Pre-immune serum (9)	5 ± 2	2 ± 1	3 ± 1

Densities are expressed as ferritin molecules per μm^2 and represent mean values ± SEM. Values in parentheses indicate the number of micrographs counted. Two representative experiments out of seven are shown to illustrate the variability in labeling density. Figs. 4–8 are taken from exp 1.

tissues initially fixed in formaldehyde; thus, this possible cause of delocalization seems unlikely.

About 100 pmol (30 μg) of antigen administered in seven divided doses over a 6-mo period were sufficient for the entire immunization of each rabbit (25). Since affinity columns could not be prepared, we compared localization of specific antibody $F(ab')_2$ (Figs. 4, 5, and 7) with the $F(ab')_2$ fraction of a pre-immunization serum (Figs. 6 and 8). These results, confirmed by quantitative morphometric analysis, indicate a highly specific reaction along the incisure of the ROS disk and the disk margin. If each disk contains approximately 10^6 rhodopsin molecules, the technique is therefore capable of determining the localization of 1–3,000 molecules of the large protein/disk. There is likely to be some amplification because of the multiplicity of ferritin molecules conjugated to the second-stage antibody and the ratio of second- to first-stage antibodies. Nonetheless, this indicates that ferritin-labeled tracers are adequate for localization of small but concentrated amounts of antigen inside cells.

The application of quantitative morphometric analysis to immunocytochemical labeling is still at an early stage. We intend to explore the variables which control labeling density in order to determine whether these techniques might be capable of measuring antigen content in a tissue. Nonetheless, it is interesting to note that the labeling density of incisures is about twice the density of margins (Table I). The result suggests that antigen on both edges of the incisure is being detected while only one antigenic edge is available at the margin. If this quantitation correctly reflects antigen density, then the plasma membrane is not likely to contain significant amounts of the large protein.

The localization to the incisure and disk margin was the result of successful immunization with a low total immunizing dose of a protein isolated from an SDS polyacrylamide gel. Because the antibodies were prepared from SDS gel purified antigens and were useful immunocytochemical reagents, this indicates that this simple approach to antigen isolation may be more generally applicable. Two-dimensional immuno-electrophoretic analysis by a highly sensitive technique was important to assess antibody specificity (25). A highly restricted anatomic locus of immunocytochemical reactions in a region of low intrinsic electron opacity after staining enhanced the contrast of the labeled sites. This technique also may be a suitable approach for study of other membrane proteins present in low molar proportions at restricted subcellular sites.

During prior biosynthetic studies of ROS membrane renewal, we noted that both opsin and the large protein are continuously synthesized and assembled into disk membranes. At the level of resolution of the kinetics of transport currently available, these two ROS proteins may be synchronously transported on membranes and assembled into disks simultaneously (24, 25). Large proteins are described in many other cells, but their binding to membranes and biosynthesis have not been extensively described. Still to be resolved is the nature of the membranes responsible for transport of these intrinsic membrane proteins from the endoplasmic reticulum and Golgi zone to the outer segment regions. It will be important to establish whether opsin and the large protein are transported in proximity to each other and with appropriate stoichiometric ratios. Alternatively, the molecular ratios and topological relationships of the final membrane may be generated during the final stages of assembly of incisures in the "free-floating" disk.

It is striking to realize that nearly all ROS disks are divided by some form of incisure so that an opsin molecule is not >0.5 μm from the nearest internal or marginal disk edge.[1] Thin ROS, such as those of human and monkey, with cross-sectional diameters of 1 μm have only shallow scalloped borders, while fish, rodent, bovine, and feline ROS are divided by one to three incisures (8, 29). The larger disks of frogs (5–7 μm) are nearly penetrated to the center by incisures (Fig. 2). The largest ROS of the mud puppy *Necturus*, which are 12 μm in diameter, are penetrated at least 3–5 μm by incisures. However, there are additional clefts inside the disk which may be homologous to the incisure and margin (4) or may

[1] The only exception to this generalization that we are aware of is that reptiles have unusually large rods, occasionally undivided by incisures. Gecko (*Coleonyx variegatus*) has a single rod divided by a single incisure (14) so that the greatest radius is 0.75 μm (corresponding to a mean collision time of 250 ms). The large undivided double and triple rods may be altered cones (31). The inner tier of photoreceptors in the cat-eyed snake (*Leptodeira annulata*) are probably rodlike in function and are 3 μm in diameter (21). Further anatomic and physiologic analysis of these unique reptilian photoreceptors may indicate their relevance to the generalization emphasized in this discussion.

be portions of tangentially sectioned incisures that are continuous from the margin to the disk interior. The purpose of incisures in ROS disks is unclear, yet their presence in one of two forms—scalloped or with a single deep cleft—throughout vertebrate life suggests that they make an important contribution to ROS function. By indenting the edge of the disk, they increase the surface area of the disk edge with little effect on the cross-sectional area available for photon capture. Because opsin molecules are mobile within the disk, collisions with these immobile regions of the disk are sufficiently frequent to retard passage of opsin across the disk from edge to edge (28).

Collisions of opsin with disk incisures and margins may be important for the functions of photoexcitation or dark adaptation. The translational diffusion constant of rhodopsin in frog ROS is approximately $3\text{–}5 \times 10^{-9}$ cm^2 s^{-1} (20, 28). This rate of diffusion may be sufficiently rapid to allow a bleached rhodopsin to reach an incisure or margin within a physiologically important time. Subsequent reactions at the restricted sites on incisures and margins may account for the changes in conductivity of the plasma membrane surrounding the disks. If the equation for a two-dimensional random walk (1) with an average dimension of 0.5 μm radius can be applied, then $t = x^2/4D$, where t is the mean collision time, x is the radius of the largest lobe of a disk, and D is the observed diffusion constant. The calculated mean collision time is between 100 and 200 ms. This is smaller than the rise time of graded potentials measured by recording the effects of single photons captured by rods (10, 33). Increased light intensity reduces the latency of the recorded potential changes, an observation which in part may be explained by the greater likelihood of light capture by a rhodopsin nearer a margin or an incisure. Alternative physiological sources of the delay of onset of the receptor potential may arise from photoreceptor coupling (15) or other metabolic events in the cell (33). One prediction of this model which couples collisions of bleached rhodopsin and incisure function is that rhodopsin would most likely act as the smallest diffusing unit possible, i.e., a monomer, to keep its diffusion time to a minimum. Another is that opsin need not function as a channel for a transmitter such as calcium ion. Rather, it may act as a receptor, which, in bleached form, could collide with a protein which constitutes a channel, thereby inducing release of a transmitter molecule. At that moment, a smaller transmitter molecule whose diffusion constant is nearer 10^{-5} cm^2 s^{-1} may be released from the disk incisures and margins and rapidly reach the plasma membrane within a few milliseconds to block sodium ion permeability and hyperpolarize the plasma membrane (10, 17, 30).

Because of the restriction of the large protein to the ROS incisure and disk margin, it becomes a potential candidate for participation in the interactions between the photoexcited disk and the hyperpolarized outer segment plasma membrane. An important test of this hypothesis would be the localization of the large protein of ROS in other species to their incisures, the determination of its function, and the localization of other functional molecules of ROS to these sites. Thus, further study of this large protein's function and biosynthesis may provide new insights into photochemical events and mechanisms of membrane assembly.

We are grateful for the helpful discussion of morphometric analysis of these data with Dr. Ewald Weibel of the Anatomy Institute, University of Bern, Switzerland, and Mr. Jeff Simonoff and Dr. John Hardigan, Yale University. We are also indebted to Dr. Max Delbruck, California Institute of Technology, Dr. Richard Cone, Johns Hopkins University, Dr. John Dowling, Harvard University, and Dr. William Miller, Yale Medical School, for their helpful discussions of rhodopsin diffusion and the speculations on incisure functions.

This work was supported in part by U. S. Public Health Service (USPHS) grants GM21714 and EY 00845, an American Cancer Society grant BC129A, the Research Center on Cellular Membranes at Yale University, and a Swiss National Science Foundation grant 3-514-75. D. Papermaster is a recipient of a USPHS Research Career Development Award, EY 00017, and during 1976–1977 was a Josiah Macy Jr. Foundation Faculty Scholar on sabbatical leave at the Department of Chemical Immunology, Weizmann Institute of Science, Rehovot, Israel.

Received for publication 17 June 1977, and in revised form 29 March 1978.

REFERENCES

1. Adams, G., and M. Delbruck. 1968. Reduction in dimensionality in biological diffusion processes. *In* Structural Chemistry and Molecular Biology. N. Davidson and A. Rich, editors. Freeman Co., New York. 198–215.
2. Basinger, S., D. Bok, and M. Hall. 1976. Rhodopsin in the rod outer segment plasma membrane. *J. Cell Biol.* **69**:29–42.

3. BROWN, P. K. 1972. Rhodopsin rotates in the visual receptor membrane. *Nat. New Biol.* **236**:35-38.
4. BROWN, P. K., I. R. GIBBONS, and G. WALD. 1963. The visual cells and visual pigment of the mud puppy, *Necturus*. *J. Cell Biol.* **19**:79-106.
5. COHEN, A. I. 1965. New details of the ultrastructure of the outer segments and ciliary connectives of the rods of human and macaque retinas. *Anat. Rec.* **152**:63.
6. COHEN, A. I. 1968. New evidence supporting the linkage to the extracellular space of outer segment saccules of frog cones but not rods. *J. Cell Biol.* **37**:424-444.
7. COHEN, A. I. 1970. Electron microscopic observations on form changes in photoreceptor outer segments and their saccules in response to osmotic stress. *J. Cell Biol.* **48**:547-565.
8. COHEN, A. I. 1972. Rods and cones. *In* Handbook of Sensory Physiology: Physiology of Photoreceptor Organs. M. G. F. Fuortes, editor. Springer-Verlag, Berlin. **VII/2**:62-112.
9. CONE, R. A. 1972. Rotational diffusion of rhodopsin in the visual receptor membrane. *Nat. New Biol.* **236**:39-43.
10. CONE, R. A. 1973. The internal transmitter model for visual excitation: some quantitative implications. *In* Biochemistry and Physiology of Visual Pigments. H. Langer, editor, Springer-Verlag New York, Inc., New York. 275-284.
11. CONE, R. A., and M. M. POO. 1973. Diffusion of rhodopsin in photoreceptor membranes. *Exp. Eye Res.* **17**:503-510.
12. CONVERSE, C. A., and D. S. PAPERMASTER. 1975. Membrane protein analyses by two-dimensional immunoelectrophoresis. Science (*Wash. D. C.*). **189**:469-472.
13. DE ROBERTIS, E., and A. LASANSKY. 1961. Ultrastructure and chemical organization of photoreceptors. *In* The Structure of the Eye. G. K. Smelser, editor. Academic Press, Inc., New York. 29.
14. DUNN, R. F. 1966. Studies on the retina of the Gecko, *Coleonyx Variegatus* I. The visual cell classification. *J. Ultrastruct. Res.* **16**:651-671.
15. FAIN, G. L., G. H. GOLD, and J. E. DOWLING. 1976. Receptor coupling in the toad retina. *Cold Spring Harbor Symp. Quant. Biol.* **40**:547-561.
16. FALK, G., and P. FATT. 1969. Distinctive properties of the lamellar and disc edge structures of the rod outer segment. *J. Ultrastruct. Res.* **28**:41-60.
17. HAGINS, W. A. 1972. The visual process: Excitatory mechanisms in the primary receptor cells. *Ann. Rev. Biophys. Bioeng.* **1**:131-158.
18. JAN, L. Y., and J. P. REVEL. 1974. Ultrastructural localization of rhodopsin in the vertebrate retina. *J. Cell Biol.* **62**:257-273.
19. KUHN, H., J. H. COOK, and W. J. DREYER. 1973. Phosphorylation of rhodopsin in bovine photoreceptor membranes. A dark reaction after light illumination. *Biochemistry*. **12**:2495-2502.
20. LIEBMAN, P. A., and G. ENTINE. 1974. Lateral diffusion of visual pigment in photoreceptor disk membranes. *Science* (*Wash. D. C.*). **185**:457-459.
21. MILLER, W. H., and SNYDER, A. W. 1977. The tiered vertebrate retina. *Vision Res.* **17**:239-255.
22. NICOLSON, G. L., and R. G. PAINTER. 1973. Anionic sites of human erythrocyte membranes. II. Anti spectrin-induced transmembrane aggregation of the binding sites for positively charged colloidal particles. *J. Cell Biol.* **59**:395-406.
23. PAPERMASTER, D. S., C. A. CONVERSE, and S. S. COPPOCK. 1976. Membrane protein assay. *Science* (*Wash. D. C.*). **192**:616.
24. PAPERMASTER, D. S., C. A. CONVERSE, and J. SIU. 1975. Membrane biosynthesis in the frog retina: opsin transport in the photoreceptor cell. *Biochemistry*. **14**:1343-1352.
25. PAPERMASTER, D. S., C. A. CONVERSE, and M. A. ZORN. 1976. Biosynthetic and immunochemical characterization of a large protein in frog and cattle rod outer segment membranes. *Exp. Eye Res.* **23**:105-116.
26. PAPERMASTER, D. S., and W. J. DREYER. 1974. Rhodopsin content in the outer segment membranes of bovine and frog retinal rods. *Biochemistry*. **13**:2438-2444.
27. PAPERMASTER, D. S., B. G. SCHNEIDER, M. A. ZORN, and J. P. KRAEHENBUHL. 1978. Immunocytochemical localization of opsin in outer segments and Golgi zones of frog photoreceptor cells. An electron microscope analysis of cross-linked albumin-embedded retinas. *J. Cell Biol.* **77**:196-210.
28. POO, M. M., and R. A. CONE. 1974. Lateral diffusion of rhodopsin in the photoreceptor membrane. *Nature* (*Lond.*). **24**:438-441.
29. STEINBERG, R. H., and I. WOOD. 1975. Clefts and microtubules of photoreceptor outer segments in the retina of the domestic cat. *J. Ultrastruct. Res.* **51**:397-403.
30. TOMITA, T. 1970. Electric activity of vertebrate photoreceptors. *Q. Rev. Biophys.* **3**:179-185.
31. WALLS, G. L. 1963. The vertebrate eye and its adaptive radiation. Hafner, New York. 607-640.
32. WEIBEL, E. R., and R. P. BOLENDER. 1973. Stereological techniques for electron microscopic morphometry. *In* Principles and Techniques of Electron Microscopy. Vol. III. M. A. Hayat, editor, Van Nostrand Reinhold Co., New York. 237.
33. YAU, K.-W., T. D. LAMB, and D. A. BAYLOR. 1977. Light-induced fluctuations in membrane current of single toad rod outer segments. *Nature* (*Lond.*). **269**:78-80.
34. YOUNG, R. W. 1971. The renewal of rod and cone outer segments in the rhesus monkey. *J. Cell Biol.* **49**:303-318.